NIH Public Access
Author Manuscript
Dev Biol. Author manuscript; available in PMC 2015 September 15.

Published in final edited form as:
Dev Biol. 2014 September 15; 393(2): 270–281. doi:10.1016/j.ydbio.2014.07.003.

Dynamics of BMP Signaling in Limb Bud Mesenchyme and Polydactyly

Jacqueline L. Norrie[1], **Jordan P. Lewandowski**[1], **Cortney M. Bouldin**[2,3], **Smita Amarnath**[1], **Qiang Li**[1], **Martha S. Vokes**[1], **Lauren I. R. Ehrlich**[1], **Brian D. Harfe**[2], and **Steven A. Vokes**[1,†]

[1]Department of Molecular Biosciences, Institute for Cellular and Molecular Biology, University of, Texas at Austin, 2500 Speedway Stop A4800 Austin, TX 78712 USA

[2]Department of Molecular Genetics and Microbiology, College of Medicine, UF Genetics, Institute, 2033 Mowry Road, Gainesville, Florida 32610

Abstract

Mutations in the Bone Morphogenetic Protein (BMP) pathway are associated with a range of defects in skeletal formation. Genetic analysis of BMP signaling requirements is complicated by the presence of three partially redundant BMPs that are required for multiple stages of limb development. We generated an inducible allele of a BMP inhibitor, *Gremlin*, which reduces BMP signaling. We show that BMPs act in a dose and time dependent manner in which early reduction of BMPs result in digit loss, while inhibiting overall BMP signaling between E10.5 and E11.5 allows polydactylous digit formation. During this period, inhibiting BMPs extends the duration of FGF signaling. *Sox9* is initially expressed in normal digit ray domains but at reduced levels that correlate with the reduction in BMP signaling. The persistence of elevated FGF signaling likely promotes cell proliferation and survival, inhibiting the activation of *Sox9* and secondarily, inhibiting the differentiation of *Sox9*-expressing chondrocytes. Our results provide new insights into the timing and clarify the mechanisms underlying BMP signaling during digit morphogenesis.

Keywords

BMP; limb development; FGF; chondrogenesis; Sox9; polydactyly; Gremlin

INTRODUCTION

Digit specification occurs within a complicated milieu of signaling pathways. Ultimately, the formation of digits is the product of regulated growth and patterning that initiate and modulate chondrogenic regulatory networks (Lopez-Rios et al., 2012; Sheth et al., 2012; Towers et al., 2008). Mutations in a surprisingly large number of genes cause the formation

© 2014 Elsevier Inc. All rights reserved.

†Corresponding author: svokes@austin.utexas.edu, Phone: 512-232-8359 Fax: 512-471-2149.
[3]Current Address: Department of Biochemistry, University of Washington, Health Sciences Building, Seattle, WA 98195

Publisher's Disclaimer: This is a PDF file of an unedited manuscript that has been accepted for publication. As a service to our customers we are providing this early version of the manuscript. The manuscript will undergo copyediting, typesetting, and review of the resulting proof before it is published in its final citable form. Please note that during the production process errors may be discovered which could affect the content, and all legal disclaimers that apply to the journal pertain.

NIH-PA Author Manuscript
NIH-PA Author Manuscript
NIH-PA Author Manuscript

NIH-PA Author Manuscript

NIH-PA Author Manuscript

NIH-PA Author Manuscript

of extra digits (polydactyly) (Biesecker, 2011). Most of these genes likely perturb the activity or output of a core signaling network that regulates proliferation and patterning in the limb bud. One of the defining features of the network is a set of iterative interactions between the limb mesenchyme and apical ectodermal ridge (AER) (Rabinowitz and Vokes, 2012).

The AER, a structure formed at the distal intersection of the dorsal and ventral ectoderm, expresses four FGF genes (*Fgf4, Fgf8, Fgf9, Fgf17*). These genes are redundant but Fgf8 is the most important, as it is widely expressed and can maintain relatively normal limb development even in the absence of the other three genes (Lewandoski et al., 2000; Mariani et al., 2008). AER FGFs are involved in promoting distal fates as well as in mediating several processes during limb development: sculpting morphology, promoting cell survival, and regulating cell velocity (Cooper et al., 2011; Gros et al., 2010; Mariani et al., 2008; Rosello-Diez et al., 2014; Sun et al., 2002; Verheyden et al., 2005).

In contrast to the actions of FGF proteins, BMP ligands are required for differentiation, where they promote exit from the cell cycle and, in the digits, chondrogenic fates (Benazet et al., 2012; Lopez-Rios et al., 2012). Three BMP proteins (BMP2, 4 and 7) are expressed in the limb with BMP4 exhibiting the most central role in digit patterning (Bandyopadhyay et al., 2006; Benazet et al., 2009; Selever et al., 2004). BMPs work in part by promoting compaction of mesodermal cells into cartilage elements (Barna and Niswander, 2007). In the complete absence of BMP activity, cartilage cells do not form in the autopod, resulting in a lack of digit formation (Benazet et al., 2012). Limb buds containing reduced levels of BMP activity often have varying degrees of digit loss, suggesting that BMP activity promotes digit formation (Badugu et al., 2012; Bandyopadhyay et al., 2006; Ovchinnikov et al., 2006). On the other hand, conditional inactivation of *Bmp4* after the limb bud has initiated results in polydactylous limbs (Benazet et al., 2009; Selever et al., 2004). One proposed explanation for these contradictory phenotypes is that BMP4 mutations result in a feedback loop triggering upregulation of overall BMP (Badugu et al., 2012). Alternatively, lowered BMP4 signaling downregulated total BMP levels, suggesting that reductions in BMPs actually promote the formation of extra digits.

Not surprisingly, BMP activity within the limb bud is tightly regulated. Posteriorly expressed Sonic hedgehog (SHH) causes the upregulation of the BMP inhibitor Gremlin (GREM1) (Eimon and Harland, 1999; Hsu et al., 1998). In the absence of GREM1 activity, BMP signaling is prematurely upregulated in the limb bud, resulting in the formation of fewer digits (Benazet et al., 2009; Khokha et al., 2003; Michos et al., 2004). Conversely, introduction of a GREM1-expressing virus in chick limb buds, results in the increased limb growth and a lack of cartilage formation (Scherz et al., 2004).

Given the central role that GREM1 plays in regulating BMP activity, it is not surprising that the correct temporal termination of *Grem1* is critical for terminating digit growth and initiating chondrogenesis. *Grem1* is normally down-regulated in the distal limb by high levels of AER-derived FGFs (Verheyden and Sun, 2008). In addition, the descendants of SHH-producing cells do not express *Grem1* (Scherz et al., 2004). *Grem1* is also repressed by direct transcriptional inputs from GLI3 and TBX2 in the anterior and posterior margins of

NIH-PA Author Manuscript

NIH-PA Author Manuscript

NIH-PA Author Manuscript

the limb, respectively (Farin et al., 2013; Li et al., 2014; Litingtung et al., 2002; te Welscher et al., 2002; Vokes et al., 2008).

In this study, we have generated a Cre-inducible allele of *Grem1* and used it to temporally inhibit BMP activity in the developing limb bud. Reduced levels of mesodermal BMPs over a defined time interval result in polydactylous hindlimbs. The polydactyly is preceded by enhanced rates of proliferation that correlate with persistent FGF activity. Although the first digit rays initiate normally, they have reduced levels of SOX9 and delayed differentiation. This results in persistent populations of undifferentiated chondrocytes at the anterior and posterior margins of the limb bud. We suggest that the delayed differentiation of these populations is likely due to the combined influences of reduced BMP activity along with upregulated FGF activity.

RESULTS

Activation of an inducible *Gremlin* allele results in polydactyly

In order to inhibit overall BMP signaling within the limb we decided to generate a Cre-inducible knock-in allele that would allow us to misexpress Gremlin, a secreted protein that has previously been shown to inhibit all limb BMPs (BMP2, 4 and 7) (Eimon and Harland, 1999; Hsu et al., 1998). Mice containing the $Rosa^{Gremlin}$ allele (hereafter referred to as RG) were crossed with a limb specific Cre, *Prx1Cre* (Logan et al., 2002), to induce ectopic *Gremlin* expression throughout the limb mesenchyme. *Gremlin* is endogenously expressed in a distinct crescent in the limb bud (Fig. 1A) while $PrxCre^{+/-};Rosa^{Gremlin/+}$ (henceforth referred to as 'Prx-RG') embryos expressed *Gremlin* broadly throughout the mesenchyme in a pattern superimposed on the endogenous domain (Fig. 1B). Prx-RG embryos activate *Gremlin* in the limb mesenchyme but not in the overlying AER, which also expresses BMPs. By E11.5, Prx-RG limb buds had significantly reduced levels of phosphorylated SMAD 1/5/8 proteins, and this inhibition persisted at least until E16.5 (Fig. 1C). Expression of the BMP target gene *Msx2* (Lallemand et al., 2005; Pizette et al., 2001) was reduced by approximately 70% at E11.75 when quantified by qRT-PCR (Fig. 1F). When visualized by in situ hybridization, *Msx2* was strongly reduced in the mesenchyme with some expression persisting in the AER (Fig. 1D–E). BMPs have previously been shown to auto-regulate their expression in the limb bud (Khokha et al., 2003; Michos et al., 2004). Consistent with these reports, *Bmp4* and *Bmp7* have significantly increased expression in Prx-RG limb buds (Fig. S1). We conclude that the Prx-RG allele has significant reductions in BMP signaling activity in the hindlimb mesoderm.

To determine the result of reduced BMP levels, we examined Prx-RG skeletal preparations. The majority of Prx-RG embryos lacked forelimbs, containing only some residual cartilage attached to the scapula (7/10 embryos; Fig. S2K). Of the remaining embryos, two had reduced numbers of digits on both forelimbs while the third had polydactyly on both forelimbs (Table S1). The forelimb phenotype was grossly evident at E11.5, with shriveled limb buds containing only small patches of AER and an absence of *Shh* expression (Fig. S2F–J, L–P). These phenotypes are consistent with previous reports indicating a transient early role for BMP signaling in AER formation (Ahn et al., 2001; Benazet and Zeller, 2013; Pajni-Underwood et al., 2007; Pignatti et al., 2014). We speculate that there is variability in

NIH-PA Author Manuscript

NIH-PA Author Manuscript

NIH-PA Author Manuscript

the onset of *Prx-Cre* activity, as a later onset would explain why 3 embryos formed digits in the forelimbs. In contrast, the hindlimbs were completely formed with normally patterned stylopod and zeugopod elements (Fig. S2A, B). The difference in phenotypes between the forelimb and hindlimb is likely caused by the earlier activation of the *Prx-Cre* transgene in the forelimb relative to the hindlimb (Logan et al., 2002). This would in turn inhibit BMP signaling at an earlier stage in forelimb development when the AER still requires BMPs. The autopods had fully penetrant soft tissue syndactyly and polydactyly that ranged from 6–9 digits (mean=7.2; SD=0.92, n=10 embryos; Fig. 1G–J; S2 A,B; Table S1). All embryos had a transformation of digit 1 ('big toe') from a shorter digit with 2 phalanges to a longer digit with 3 phalanges. Digits from RG embryos were significantly shorter than their wild type counterparts and they were also more uniform in length (Fig. S2C, D). Each of the individual metatarsal and phalange elements comprising the shortened digits were proportionally reduced, indicating that this is a general shortening of the digit (Fig. S2D). Compared to sibling controls, the phalanges had delays in ossification that were most pronounced at the digit tips (Fig. 1I,J). Similar delays were noted in the posterior regions of *ShhCre*$^{+/-}$;*RG* digits (Fig. S3A–D; Table S2), indicating that polydactyly can occur in both the anterior and posterior margins.

Temporal window for BMP-dependent regulation of digit number

Inhibiting BMPs could potentially cause polydactyly during a wide developmental time window. To determine the temporal range, we analyzed RG embryos containing *HoxB6CreER*, a tamoxifen-inducible Cre that has activity throughout hindlimb mesoderm (Nguyen et al., 2009). This approach allowed us to assay embryos expressing either one or two copies of RG (abbreviated as HoxB6CreER-RG or HoxB6CreER-RG/G, respectively). As a control, we established that siblings that did not contain HoxB6CreER (but also received tamoxifen) had normal, pentadactylous limbs. While we report phenotypes for the forelimb skeletal preparations (Fig. S4; Table S3), we focused on the hindlimb because HoxB6CreER is only active in the posterior portion of the forelimb (Nguyen et al., 2009). To determine the range over which BMPs regulate digit number, we injected pregnant mice at 12-hour intervals between E9.5 and E11.5. The *HoxB6CreER* mouse line causes efficient recombination at the *Rosa26* locus between 8–12 hours after Tamoxifen injection (Nguyen et al., 2009; Zhu et al., 2008); the interval between tamoxifen injection and the onset of BMP inhibition is represented by the white bars in Fig. 2A. Overall, hindlimbs from embryos containing two copies of RG had more severe phenotypes than those with one copy, indicating that the phenotype is dose-responsive. When tamoxifen was injected at E9.5, HoxB6CreER-RG/G hindlimbs were either normal (2/5; Table S3) or had a loss of nearly the entire limb, containing only a few digit-like elements (3/5; Fig. 2B,G; Table S3). The loss of hindlimbs in these embryos was similar to the loss of forelimbs in Prx-RG embryos (Fig. S2K), suggesting that this defect was caused by inhibiting BMPs during their early role in AER formation. As administration of tamoxifen at later stages resulted in polydactyly, it is not clear why a subset of these hindlimbs were normal at this stage. When injections were performed at E10.0 and E10.5, all HoxB6CreER-RG/G embryos had polydactyly (Table S3; Fig. 2H, I). As observed in Prx-RG, this included a transformation of digit one from two phalanges to three phalanges. Some HoxB6CreER-RG/G embryos from E10 (5/8) and E10.5 (2/3) injections also had bowed femurs and tibia with a reduced or

NIH-PA Author Manuscript

NIH-PA Author Manuscript

NIH-PA Author Manuscript

absent fibula (Fig. 2I, arrowhead). When injected at E11, HoxB6CreER-RG/G embryos had multiple bifurcated digits (n=3/3) but there were no completely formed extra digits. HoxB6CreER-RG embryos contained nubs or, in one case, bifurcated digits (Fig. 2 E,J; Table S3). Embryos injected at E11.5 contained a posterior skin nub that was smaller than nubs observed at when the transgene was activated earlier in development. The *HoxB6CreER* transgene is no longer expressed throughout the hindlimb after E11.5 but additional experiments using the ubiquitous $Rosa^{Cre\text{-}ERT2}$ (Ventura et al., 2007), which is expressed ubiquitously upon tamoxifen activation, indicated that $Rosa^{Cre\text{-}ERT2/Gremlin}$ embryos did not form nubs or polydactyly after E11.5 (Table S4). Because of the ~12 hour delay between injection and activation, we conclude that BMPs regulate digit number between E10.5–11.5.

BMP inhibition results in persistent, amplified FGF signaling

To determine how *Gremlin* mis-expression and BMP inhibition affected early limb patterning, we determined the expression patterns for *Shh* and FGF response. At E11.5, Prx-RG hindlimbs have expanded anterior and posterior expression of *Fgf4* and *Fgf8* (Fig. 3A, B, E, F). There also appears to be a slight increase in expression of the FGF target gene *Spry4* (Fig. 3I,J). The domain of Shh expression is also expanded along the proximal to distal axis, consistent with previously described roles for BMPs in negatively regulating *Shh* (Bastida et al., 2009) (Fig. 3 M–N). By E12.5, wild type hindlimbs have normally lost *Fgf4* and *Shh* but their expression persists in Prx-RG hindlimbs (Fig. 3C,D,O,P). In addition, *Fgf8* and *Spry4* are expressed at higher levels than control embryos (Fig. 3G,H,K,L). To quantify these observations, we assayed gene expression in E11.75 limb buds by quantitative RT-PCR (Fig. 3Q–T). Consistent with the expression data, there are significant increases in *Shh, Fgf8* and the FGF responsive genes *Dusp6* and *Spry4* (Kawakami et al., 2003; Mariani et al., 2008; Minowada et al., 1999; Verheyden and Sun, 2008). We conclude that Prx-RG hindlimbs have elevated, sustained levels of FGF signaling.

Inhibiting BMPs results in enhanced proliferation and reduced apoptosis

The increased size of Prx-RG was initially apparent by E11.5 (Fig. 3) while there is a large difference by E12.5. This increased size could be caused by increased proliferation rates and/or reduced levels of apoptosis. To determine if there were changes in proliferation, we first examined the percentage of cells in mitosis using an antibody against phosphohistone H3 that recognizes cells in late G2 and mitosis (Hendzel et al., 1997). We focused our analysis to embryos between 45–47 somites, shortly after size differences between wild type and Prx-RG hindlimbs are apparent (Fig. 3). Autopods from Prx-RG hindlimbs had a 20% increase in their mitotic index (8.6% in sibling controls compared to 10.4% in Prx-RG $P<0.002$) (Fig. 4A–C) indicating an increase in the percentage of proliferating cells.

We then measured proliferation by flow cytometry using hindlimb autopods from 45–49 somites. There was no difference in the percentage of cells in G0/1, S or G2/M (Fig. 4D–F). At E12.5, the percentage of cells in G0/1, S or G2/M was comparable in percentage to the E11.75 (45–49 somite) sample (Fig. S5C–E). Prx-RG hindlimbs did not have upregulated *Cdk6* expression as has previously been noted in $Gli3^{-/-}$ forelimbs (Lopez-Rios et al., 2012). Similarly, Prx-RG hindlimbs did not have upregulated *Axin2* expression, suggesting

NIH-PA Author Manuscript

NIH-PA Author Manuscript

NIH-PA Author Manuscript

that canonical Wnt signaling was not elevated (Fig. S5A,B). The discrepancy between these results and the increase observed in the mitotic index are discussed in the Discussion.

We examined changes in apoptosis using Lysotracker Red, an established marker of apoptotic cells in the limb bud (Fogel et al., 2012; Zhu et al., 2008). At E11.75, Prx-RG autopods have reduced levels apoptosis in the anterior AER and mesoderm (n=6) compared to sibling controls (Fig. 4G,H; n=3). By E12.5, many apoptotic cells are present in the posterior AER and the anterior necrotic zone in control hindlimbs (Fig. 4I; n=6). Apoptotic cells in the posterior zone are strongly reduced in Prx-RG limb buds. In addition the normal anterior necrotic zone (outlined arrowhead in 4I) is completely absent with a new apoptotic domain expressed in a more proximal anterior position (asterisk in Fig. 4J; n=3). We conclude that Prx-RG hindlimbs have enhanced levels of proliferation while having reduced levels of apoptosis.

Reduced BMP levels result in delayed digit formation

To determine the onset of digit formation in Prx-RG hindlimbs, we examined the expression of *Sox9*, the earliest known marker of future chondrocytes, and *Col2a1*, a marker of differentiated chondrocytes that is a direct transcriptional target of SOX9 (Bell et al., 1997; Oh et al., 2010). At E12.5, wild type embryos expressed both *Sox9* and *Col2a1* in all five digit rays in contralateral hindlimbs (Fig. 5A,B). At this stage, Prx-RG embryos had an average of 4.6 *Col2a1*-expressing rays while they had an average of 5.8 *Sox9* expressing rays in their contralateral hindlimbs ($P<0.05$ Paired T-Test). In addition to having a delayed onset in *Col2a1* expression in some digits, digit ray formation was still ongoing in Prx-RG embryos at this stage, as they ultimately formed an average of 7.2 polydactylous digits (Fig. 5C,D). The persistence of forming digits could be the result of developmental delay. To address this, we examined digit formation at earlier stages of development. Wild type hindlimbs at E11.75 had three fully resolved *Sox9*-expressing digit rays as did similarly staged Prx-RG embryos (Fig. 5E,F), suggesting that initial digit ray formation was not delayed. However, Prx-RG hindlimbs had reduced levels of *Sox9* mRNA and SOX9 protein expression (Fig. 5G,K) and *Sox9*-expressing digit rays were significantly restricted from the most distal autopod in Prx-RG embryos (Fig 5E,F). Sibling control embryos had an average domain of 112 μm between the boundary of *Sox9* expression and the AER while Prx-RG embryos had an average boundary of 144 μm ($P<0.05$). Together, these experiments suggested that Prx-RG embryos formed digit rays at a comparable rate to wild type controls albeit with more truncated domains. They also suggest that digit development persisted for a longer in the anterior and posterior margins that gave rise to most polydactylous digits.

To examine this phenotype more closely, we examined SOX9 protein expression by immunostaining in sectioned RG hindlimbs. Consistent with the reduced levels of *Sox9* mRNA, SOX9 expression levels were significantly reduced both in fully resolved digit rays and pre-condensed regions (Fig. 5I–K,M,N). At this stage, wild type digit rays have more densely packed chondrocytes than Prx-RG rays (Fig. 5I,M,O) while chondrocytes that have not yet formed rays appear to have similar densities in wild type and Prx-RG embryos (Fig. 5J,N,O). The reduced levels of SOX9 and delayed compaction in Prx-RG embryos suggest

NIH-PA Author Manuscript

NIH-PA Author Manuscript

NIH-PA Author Manuscript

that they have delays in later chondrogenesis although they initially form digit rays at a rate that is comparable to wild type embryos.

Reduced BMP and enhanced FGF signaling delay chondrogenic differentiation

The preceding experiments suggested that Prx-RG hindlimbs digit rays were specified normally but might have delays in chondrocyte differentiation. This delay could be caused by threshold reductions in BMP signaling required to promote digit chondrogenesis; alternatively, the persistently elevated levels of FGF signaling present in Prx-RG hindlimbs (Fig. 3) could inhibit chondrogenesis as has been shown in cultured limb bud mesenchyme (Cooper et al., 2011; Lewandowski et al., 2014; ten Berge et al., 2008). This possibility is consistent with the distal truncations in *Sox9* expressing digits observed above. To test the roles of BMP and FGFs in more detail, we cultured wild type and Prx-RG hindlimb autopods under micromass-like conditions in control media or in media containing FGF8, BMP4, or both (Fig. 6A). After 24 hours of culture under control conditions, Prx-RG had a 51% reduction in the BMP target gene *Msx2* and a 35% reduction in *Sox9* compared to wild type cultures (Fig. 6B,C). In addition, Prx-RG cultures also had reductions in the chondrocyte differentiation markers *Agc1* and *Col9a1* (Fig. 6D,E) (Bi et al., 1999; Sekiya et al., 2000; Zhang et al., 2003). These results are consistent with the reduced levels of chondrogenic markers and delayed differentiation observed in embryonic limb buds (Figs. 5G, 1F).

The addition of FGF8 to the media caused significant reductions in *Msx2* expression while *Sox9, Agc1* and *Col9a1* were not significantly changed in Prx-RG hindlimb cell cultures when compared to control conditions (Fig. 6B–E). As expected, the addition of BMP4 to the media caused significant increases in *Msx2* as well as *Sox9, Agc1* and *Col9a1*. Conversely, these same markers are all reduced in the lowered BMP environment present in cultured Prx-RG samples compared to wild type samples. These results are consistent with the in vivo results (Fig. 5) and suggest that BMP regulates *Sox9* in the autopod. Compared to the addition of BMP4 alone, cultures of wild type hindlimbs treated with BMP4 and FGF8 had comparable levels of *Msx2* and *Sox9* but strongly reduced levels of *Agc1* and *Col9a1* (Fig. 6B–E). In this set of conditions, co-administration of FGF8 did not significantly inhibit Sox9 or BMP response (as measured by *Msx2*) yet strongly inhibited the activation of differentiation markers. This raises the possibility that an FGF-responsive protein could inhibit transcription of chondrocyte differentiation genes through a SOX9-independent mechanism (see Discussion, Fig. 7). In summary, these experiments suggest that both the reduced BMP signaling levels as well as increased FGF levels contribute to delays in chondrogenesis.

DISCUSSION

Reduced mesodermal BMP signaling levels result in increased digit number

In this study we have examined the effect of reducing BMP levels in the limb mesenchyme using a Cre-inducible construct that activates *Gremlin* (Fig. 1A–F). We show that BMPs act in a dose and time dependent manner in which early or complete loss of BMPs result in digit loss, but inhibiting overall BMP signaling between E10.5 and E11.5 causes polydactylous

NIH-PA Author Manuscript

NIH-PA Author Manuscript

NIH-PA Author Manuscript

digit formation (Fig. 2). RG hindlimbs have many phenotypes consistent with a loss of BMP signaling including ectopic *Fgf4* expression, expanded *Shh* expression and delayed AER regression (Bandyopadhyay et al., 2006; Bastida et al., 2009; Benazet et al., 2012; Pizette and Niswander, 1999; Verheyden and Sun, 2008). We were initially surprised that RG embryos ultimately form digits, as previous studies overexpressing BMP inhibitors resulted in an absence of cartilage formation (Capdevila et al., 1999; Lopez-Rios et al., 2012; Pizette et al., 2001; Scherz et al., 2004). The most likely explanation is that in the RG allele BMP levels are reduced but not below a threshold level required for digit specification. Consistent with the idea the RG activation results in sustained inhibition of BMP signaling, BMP-specific pSMAD levels are decreased by ~50% in E11.5 Prx-RG hindlimbs and by ~30% in E16.5 autopods (Fig. 1C). While the E16.5 autopod contains multiple differentiated cell types, the decrease in pSMAD inhibition suggests that BMP signaling has partially compensated for the presence of a steady-state inhibitor. If there is feedback compensation, BMP signaling might transiently be reduced to greater levels than indicated by overall protein levels on western blots.

In addition to their mesodermal roles, BMPs are also expressed in the AER where they are transiently required for its formation (Ahn et al., 2001; Barrow et al., 2003; Benazet et al., 2012; Benazet and Zeller, 2013; Choi et al., 2012; Pizette et al., 2001). The mesodermal activation of *Gremlin* prior to ~E10.5 leads to severe reductions in limb growth and digit number that are consistent with this secreted protein providing localized disruption to the AER (Fig, S2, 2G). While some conditional mutations in BMP result in digit reductions, mutations in BMP4 are polydactylous (Benazet et al., 2009; Dunn et al., 1997; Selever et al., 2004). Our results strongly suggest that the polydactyly seen in conditional deletions of BMP4 in the mesoderm are caused by overall reductions in BMP signaling levels and not by compensatory upregulation of other BMPs (Badugu et al., 2012).

Increased proliferation and reduced apoptosis in RG hindlimbs

At E11.5, near the onset of appreciable size difference between RG hindlimbs and controls, the mitotic index had a 20% overall increase in rate in RG hindlimbs (Fig 4A–C). We do not detect any difference in G0/1, S or G2/M in similarly staged limb buds by FACS at either E11.75 or E12.5 (Figs. 4D–F; S5C–E). The mitotic index is likely a more sensitive method of detecting small changes in the G2/M phase while the lack of accompanying changes in the percentage of S-phase cells suggests that there could be changes in cell cycle rate. Consistent with this possibility, the most distal limb bud cells are reported to have decreased cell cycle times compared to the rest of the limb in wild type embryos (Boehm et al., 2010).

FGF8 does not cause increased proliferation in cultured limb bud mesenchyme, which is devoid of most or all ectoderm, but it does enhance proliferation when co-cultured with either Wnt3a or Hedgehog activators (Lewandowski et al., 2014; ten Berge et al., 2008). Wnt ligands are expressed in the ectoderm where they act as mitogens on the adjacent mesoderm (ten Berge et al., 2008). If FGF8 plays a similar enhancing role *in vivo*, this effect should be most pronounced between E11.5–12.5 when there is normally a sharp reduction in FGF activity (Fig. 3I,K). This correlates with period when there is an increase in size in the autopods of RG hindlimbs compared to controls (Fig. 3), and is consistent with the idea that

NIH-PA Author Manuscript

NIH-PA Author Manuscript

NIH-PA Author Manuscript

persistent FGFs are causing an increase in proliferation. The increase in mitotic index in our study (Fig 4A–C) but unchanged percentage of S-phase cells in RG limb buds contrasts with the enhanced anterior proliferation associated with anterior polydactyly in *Gli3*$^{-/-}$ limb buds, in which an enhanced G1-S transition is likely mediated by elevated CDK6 with no change in mitotic index (Lopez-Rios et al., 2012). Supporting the notion that RG limb buds have different drivers of proliferation, we also do not observe a change in *Cdk6* levels (Fig. S5A).

An alternative interpretation of our data is that despite the increased mitotic index, proliferation is not a major driver of the increased size seen in RG limb buds. Computational simulations by Boehm et al suggest that increased proliferation rates do not play a role in normal distal limb development. Instead, they propose that limb growth is caused by directional cell behaviors(Boehm et al., 2010). FGF signaling has been shown to promote cell velocity in the early limb bud (Gros et al., 2010) and could potentially continue to promote increased velocity this later phase of limb bud growth that could affect the increased size of the digit paddle. In addition to increased proliferation, RG hindlimbs have reduced apoptosis that is most pronounced in the anterior mesoderm (Fig. 4G–J). Apoptosis plays important roles in sculpting the autopod domain and reduced levels have classically been associated with polydactyly (Kimura and Shiota, 1996; Milaire and Rooze, 1983). Although we did not quantify apoptosis within the inter-digit mesenchyme of later limb buds, the webbing present in RG hindlimbs (Fig. 1H) indicates a loss of apoptosis in this domain as well. This is consistent with other studies that have shown that persistent, elevated FGF signaling in the AER counteracts BMP-induced apoptosis (Lu et al., 2006; Pajni-Underwood et al., 2007).

The role of BMP signaling in digit specification

In the absence of Smad4 within the autopod, digit rays fail to form and *Sox9* is not expressed, implying a requirement for BMP signaling (Benazet et al., 2012). Based on this data, BMPs could either act upstream of *Sox9* to initiate transcription or they could provide a permissive environment in which *Sox9* would subsequently be activated. By reducing BMP activity, we do not observe significant delays in the onset of *Sox9*-expressing digit rays (Fig. 5E,F) but there are significant reductions the levels of *Sox9* mRNA and protein (Fig. 5G,K). This suggests that once BMP has reached a previously hypothesized threshold necessary for *Sox9* activation (Bandyopadhyay et al., 2006), it then regulates its expression in a dose-dependent fashion. In cultured limb bud mesenchyme we observe a similar trend with BMP4 causing a significant upregulation of *Sox9* that is dampened in RG cultures (Fig. 6C). Although we do not observe delays in the onset of *Sox9* expression in the autopod, the reduced levels of SOX9 protein likely result in the observed delay in activating the SOX9 target gene *Col2a1*. The delay suggests that SOX9 activity in RG embryos must reach threshold levels of activity before activating differentiation markers.

FGFs inhibit chondrogenic differentiation

Because RG limb buds have high levels of FGF signaling, we sought to determine how it influences chondrogenesis. Previous studies have shown that FGF signaling delays chondrogenesis in cultured limb bud mesenchyme (Cooper et al., 2011; Lewandowski et al.,

NIH-PA Author Manuscript

NIH-PA Author Manuscript

NIH-PA Author Manuscript

2014; ten Berge et al., 2008). FGF signaling activity is highest in the distal mesoderm, suggesting that the truncated digit rays in RG embryos are caused by direct or indirect repression of *Sox9* (Fig 5F). Interestingly, autopod cultures containing both BMP4 and FGF8 had significant reductions in the transcription of the cartilage differentiation marker *Agc1* compared to cultures treated only with BMP4. These cultures did not have significant reductions in the BMP-responsive gene *Msx2* or *Sox9*, which is already expressed in limb buds when they are dissected (Fig. 6B–E). Moreover, FGF8 did not have a proliferative effect on cultures treated under identical conditions (Lewandowski et al., 2014). We speculate that FGF signaling represses *Sox9* activation by maintaining cells in a proliferative state as well as providing an independent repressive effect on the activation of chondrocyte differentiation markers that occurs in parallel to BMP-dependent activation of Sox9 (Fig 7).

Opposing actions of BMP and FGF on digit chondrogenesis

We have summarized the opposing roles for BMPs and FGFs in Fig. 7. The persistent FGF signaling in RG limb buds acts as a permissive factor to enhance cell proliferation and also provides increased cell survival in the anterior and posterior margins of the limb bud. Although BMP signaling is reduced in RG hindlimbs, it does not fall below threshold levels necessary to activate *Sox9* in the autopod. Nonetheless, *Sox9* expression is reduced within nascent chondrocytes, suggesting BMP acts as a dose dependent transcriptional regulator of *Sox9*. FGF signaling also negatively regulates chondrogenesis both by promoting cell proliferation and inhibiting differentiation of SOX9-expressing chondrocytes. We speculate that persistent FGF signaling in nascent chondrocytes upregulates a repressor of chondrogenic differentiation, depicted as “Repressor” in Fig. 7B. The HOXD13 and HOXA13 paralogues are plausible repressor candidates, as FGFs promote the activation of these distal Hox genes (Rosello-Diez et al., 2014; Vargesson et al., 2001). While HOXA13 and HOXD13 are jointly required for normal digit condensation, the overexpression of HOXD13 negatively regulates chondrogenic differentiation (Fromental-Ramain et al., 1996; Kuss et al., 2009; Stadler et al., 2001). Moreover, *Sox9* is still expressed in *HoxA13*$^{-/-}$ digits (Perez et al., 2010), consistent with our finding that the repressor seems to act in a parallel pathway. As persistent FGF signaling from the AER is a common feature of many disparate polydactylies, we propose that this model will be more generally relevant to understanding how extra digits are generated.

MATERIALS AND METHODS

Unless noted otherwise, statistical significance was measured using a two-tailed, unpaired T-test.

Creation of mouse strains and manipulation of embryos

Experiments involving mice were approved by the Institutional Animal Care and Use Committee at the University of Texas at Austin (protocol AUP-2013-00168). A mouse *Grem1* cDNA was subcloned into pBigT and targeted to the *Rosa26* locus under control of the *Rosa26* promoter in CJ7 ES cells (Srinivas et al., 2001; Swiatek and Gridley, 1993). ES cells were then injected to generate a Cre-inducible *Gremlin, RosaGremlin*, (official name is Gt(ROSA)26Sor<tm1(Grem1)Svok>; Accession ID: MGI:5561086). Embryos were

NIH-PA Author Manuscript

NIH-PA Author Manuscript

NIH-PA Author Manuscript

genotyped for the presence of the *Rosa26* knock-in allele using the following primers that generated a 315bp amplicon: 5'GCGAAG AGTTTGTCCTCAACC3' and 5' AAAGTCGCTCTGAGTTGTTAT3'. *RosaGremlin* mice were crossed to PrxCre (Logan et al., 2002), *HoxB6CreER* (Nguyen et al., 2009), *ShhCre* (Harfe et al., 2004) and RosaCreER^{T2} (Ventura et al., 2007) lines. Pregnant mice containing *HoxB6CreER* embryos were intraperitoneally injected with 3mg of Tamoxifen per 40g at specified times. In cell proliferation experiments, pregnant females were intraperitoneally injected with 2mg BrdU and embryos were collected 1 hour later. Skeletal preparations were performed on E18.5 embryos as described previously (Allen et al., 2011). Lysotracker Red staining was visualized using 1:2 benzyl alcohol:benzyl benzoate using established protocols except that limb buds were stained for 5 minutes in Lysotracker Red (Fogel et al., 2012; Zhu et al., 2008).

Western blots and immunostaining

Western blots: Ectoderm was dissected from hindlimb buds from E11.5 and E16.5 limb buds, which were homogenized in RIPA buffer containing complete mini EDTA free protease inhibitors and PhosphoSTOP (Roche). 10–15μg of each sample was run on 8% SDS PAGE gels, transferred onto nitrocellulose membranes and incubated with anti-pSMAD 1/5/8 (1:500 in 5% BSA; Cell Signaling #9511S) or anti-Actin (1:2000 in 5% Block; Sigma #A2066). Membranes were then incubated in Donkey anti-rabbit secondary and developed using ECL Prime Western Blotting Detection Reagent (GE Healthcare). Band intensities were quantified using ImageQuant software.

Immunostaining: With the exception of the panels shown in Figure 5H, L (Zeiss Axiovert Fluorescent light micropscope), samples were imaged on a Zeiss 710 confocal microscope. For detecting cells in late G2/M, limb buds were fixed in 4% paraformaldehyde for 20 minutes at room temperature. Cryosections were incubated with anti-phosphohistone H3 (1:200; Millipore #06–570), Alexa Fluor 568-conjugated goat anti rabbit secondary (1:250), and DAPI. Unless noted otherwise, confocal images collected as tiled scans with a 20X objective with a total of 4 Z-stacks over a 6μm range and processed using ZEN (Zeiss) to obtain maximum intensity projections. The total number of phosphohistone H3-expressing cells and DAPI expressing cells were counted using CellProfiler 2.0 (r11710) as described previously (Ljosa and Carpenter, 2009). Limb buds used for visualizing BrdU/Sox9 expression were cryosectioned prior to fixation in acetone for 2 min. Sections were then incubated for 30 minutes in 2M HCl, 5 minutes in Tris base, blocked for 15 minute at room temperature in TNB buffer (0.1M Tris pH 3.5, 0.15M NaCl, 0.5% Blocking solution (Roche #11096176001)) and incubated with primary antibodies (Sox9 1:500 - Millipore #AB5535; Biotin-conjugated BrdU 1:50 - Abcam #ab74547) and either Alexa Flour 568-conjugated goat anti-rabbit (1:250) or streptavidin-conjugated Dylight 488 (1:200) followed by DAPI. The fluorescence intensity of anit-Sox9 immunostaining was analyzed using MetaMorph.

Flow Cytometry Analysis

Hindlimb autopods at E11.75 (45–49 somites, 1 litter per experiment containing hindlimbs from a minimum of 3 embryos per genotype) or E12.5 (hindlimbs from 2–3 embryos per genotype per experiment) were dissected as previously described (Lopez-Rios et al., 2012).

NIH-PA Author Manuscript

NIH-PA Author Manuscript

NIH-PA Author Manuscript

Cells were prepared for analysis using the FITC BrdU Flow Kit (BD Biosciences) and sorted on an LSRII Fortessa FCM (BD Biosciences). Data was analyzed using FlowJo software.

Limb mesenchyme cultures

We used Hindlimbs from E11.5 (45–49 somites) Prx-RG and sibling controls ($PrxCre^{+/-}$). Five separate experiments were performed, and per experiment, we pooled both hindlimbs from approximately three embryos. Limb cell cultures were performed as described in (Lewandowski et al., 2014). Briefly, for each respective genotype, limb buds were trypsinized and cells were passed through a 40uM nylon filter. Dissociated limb cells were plated at approximately 150,000 cells per well on 96-well half area plates. Limb cells were cultured for 24 hours in either control media or media supplemented with 150ng/mL FGF8b (R&D Systems,), 50ng/mL BMP4 (R&D Systems), or both. At 24 hours cells were harvested, RNA was extracted using PureLink RNA mini kit (Ambion) and treated with DNAse I. cDNA was synthesized using SuperScript II with random hexamers (Invitrogen) from 250ng of total RNA.

Quantitative RT-PCR

RNA was extracted from hindlimb buds using Trizol Reagent (Life Technologies; 15596-026) and cDNA was synthesized using SuperScript II with random hexamers (Invitrogen; 18064-014) from 500ng of DNAse 1 treated total RNA. Gene expression experiments were performed on a Viia7 (ABI) platform using SensiFast SYBR Lo-Rox (Bioline). Unless specified otherwise in the figure legends (Figs. 5,6), values were normalized to beta-actin. Fold-changes in gene expression was calculated using the delta-CT method (Livak and Schmittgen, 2001). Primers used in this study are listed in Table S5.

Supplementary Material

Refer to Web version on PubMed Central for supplementary material.

Acknowledgments

We thank Dr. Benoit Robert and Dr. Chin Chiang for providing constructs, Julie Hayes in the ICMB Microscopy and Imaging Facility for advice on microscopy imaging and the ICMB Mouse Genetic Engineering Facility for blastocyst injections. We thank Simone Giovanetti for comments on the manuscript. This work was supported by NIH R01HD073151 (to S.A.V) and startup funds from the College of Natural Sciences and the Institute for Cellular and Molecular Biology at the University of Texas at Austin (to S.A.V).

REFERENCES

Ahn K, Mishina Y, Hanks MC, Behringer RR, Crenshaw EB 3rd. BMPR-IA signaling is required for the formation of the apical ectodermal ridge and dorsal-ventral patterning of the limb. Development. 2001; 128:4449–4461. [PubMed: 11714671]

Allen BL, Song JY, Izzi L, Althaus IW, Kang JS, Charron F, Krauss RS, McMahon AP. Overlapping roles and collective requirement for the coreceptors GAS1, CDO, and BOC in SHH pathway function. Dev Cell. 2011; 20:775–787. [PubMed: 21664576]

Badugu A, Kraemer C, Germann P, Menshykau D, Iber D. Digit patterning during limb development as a result of the BMP-receptor interaction. Sci Rep. 2012; 2:991. [PubMed: 23251777]

NIH-PA Author Manuscript

NIH-PA Author Manuscript

NIH-PA Author Manuscript

Bandyopadhyay A, Tsuji K, Cox K, Harfe BD, Rosen V, Tabin CJ. Genetic analysis of the roles of BMP2, BMP4, and BMP7 in limb patterning and skeletogenesis. PLoS Genet. 2006; 2:e216. [PubMed: 17194222]

Barna M, Niswander L. Visualization of cartilage formation: insight into cellular properties of skeletal progenitors and chondrodysplasia syndromes. Dev Cell. 2007; 12:931–941. [PubMed: 17543865]

Barrow JR, Thomas KR, Boussadia-Zahui O, Moore R, Kemler R, Capecchi MR, McMahon AP. Ectodermal Wnt3/beta-catenin signaling is required for the establishment and maintenance of the apical ectodermal ridge. Genes Dev. 2003; 17:394–409. [PubMed: 12569130]

Bastida MF, Sheth R, Ros MA. A BMP-Shh negative-feedback loop restricts Shh expression during limb development. Development. 2009; 136:3779–3789. [PubMed: 19855020]

Bell DM, Leung KK, Wheatley SC, Ng LJ, Zhou S, Ling KW, Sham MH, Koopman P, Tam PP, Cheah KS. SOX9 directly regulates the type-II collagen gene. Nat Genet. 1997; 16:174–178. [PubMed: 9171829]

Benazet JD, Bischofberger M, Tiecke E, Goncalves A, Martin JF, Zuniga A, Naef F, Zeller R. A self-regulatory system of interlinked signaling feedback loops controls mouse limb patterning. Science. 2009; 323:1050–1053. [PubMed: 19229034]

Benazet JD, Pignatti E, Nugent A, Unal E, Laurent F, Zeller R. Smad4 is required to induce digit ray primordia and to initiate the aggregation and differentiation of chondrogenic progenitors in mouse limb buds. Development. 2012; 139:4250–4260. [PubMed: 23034633]

Benazet JD, Zeller R. Dual requirement of ectodermal Smad4 during AER formation and termination of feedback signaling in mouse limb buds. Genesis. 2013; 51:660–666. [PubMed: 23818325]

Bi W, Deng JM, Zhang Z, Behringer RR, de Crombrugghe B. Sox9 is required for cartilage formation. Nat Genet. 1999; 22:85–89. [PubMed: 10319868]

Biesecker LG. Polydactyly: how many disorders and how many genes? 2010 update. Dev Dyn. 2011; 240:931–942. [PubMed: 21445961]

Boehm B, Westerberg H, Lesnicar-Pucko G, Raja S, Rautschka M, Cotterell J, Swoger J, Sharpe J. The role of spatially controlled cell proliferation in limb bud morphogenesis. PLoS Biol. 2010; 8:e1000420. [PubMed: 20644711]

Capdevila J, Tsukui T, Rodriquez Esteban C, Zappavigna V, Izpisua Belmonte JC. Control of vertebrate limb outgrowth by the proximal factor Meis2 and distal antagonism of BMPs by Gremlin. Mol Cell. 1999; 4:839–849. [PubMed: 10619030]

Choi KS, Lee C, Maatouk DM, Harfe BD. Bmp2, Bmp4 and Bmp7 are co-required in the mouse AER for normal digit patterning but not limb outgrowth. PLoS One. 2012; 7:e37826. [PubMed: 22662233]

Cooper KL, Hu JK, ten Berge D, Fernandez-Teran M, Ros MA, Tabin CJ. Initiation of proximal-distal patterning in the vertebrate limb by signals and growth. Science. 2011; 332:1083–1086. [PubMed: 21617075]

Dunn NR, Winnier GE, Hargett LK, Schrick JJ, Fogo AB, Hogan BL. Haploinsufficient phenotypes in Bmp4 heterozygous null mice and modification by mutations in Gli3 and Alx4. Dev Biol. 1997; 188:235–247. [PubMed: 9268572]

Eimon PM, Harland RM. In Xenopus embryos, BMP heterodimers are not required for mesoderm induction, but BMP activity is necessary for dorsal/ventral patterning. Dev Biol. 1999; 216:29–40. [PubMed: 10588861]

Farin HF, Ludtke TH, Schmidt MK, Placzko S, Schuster-Gossler K, Petry M, Christoffels VM, Kispert A. Tbx2 terminates shh/fgf signaling in the developing mouse limb bud by direct repression of gremlin1. PLoS Genet. 2013; 9:e1003467. [PubMed: 23633963]

Fogel JL, Thein TZ, Mariani FV. Use of LysoTracker to detect programmed cell death in embryos and differentiating embryonic stem cells. J Vis Exp. 2012

Fromental-Ramain C, Warot X, Messadecq N, LeMeur M, Dolle P, Chambon P. Hoxa-13 and Hoxd-13 play a crucial role in the patterning of the limb autopod. Development. 1996; 122:2997–3011. [PubMed: 8898214]

Gros J, Hu JK, Vinegoni C, Feruglio PF, Weissleder R, Tabin CJ. WNT5A/JNK and FGF/MAPK pathways regulate the cellular events shaping the vertebrate limb bud. Curr Biol. 2010; 20:1993–2002. [PubMed: 21055947]

NIH-PA Author Manuscript

NIH-PA Author Manuscript

NIH-PA Author Manuscript

Harfe BD, Scherz PJ, Nissim S, Tian H, McMahon AP, Tabin CJ. Evidence for an expansion-based temporal Shh gradient in specifying vertebrate digit identities. Cell. 2004; 118:517–528. [PubMed: 15315763]

Hendzel MJ, Wei Y, Mancini MA, Van Hooser A, Ranalli T, Brinkley BR, Bazett-Jones DP, Allis CD. Mitosis-specific phosphorylation of histone H3 initiates primarily within pericentromeric heterochromatin during G2 and spreads in an ordered fashion coincident with mitotic chromosome condensation. Chromosoma. 1997; 106:348–360. [PubMed: 9362543]

Hsu DR, Economides AN, Wang X, Eimon PM, Harland RM. The Xenopus dorsalizing factor Gremlin identifies a novel family of secreted proteins that antagonize BMP activities. Mol Cell. 1998; 1:673–683. [PubMed: 9660951]

Kawakami Y, Rodriguez-Leon J, Koth CM, Buscher D, Itoh T, Raya A, Ng JK, Esteban CR, Takahashi S, Henrique D, Schwarz MF, Asahara H, Izpisua Belmonte JC. MKP3 mediates the cellular response to FGF8 signalling in the vertebrate limb. Nat Cell Biol. 2003; 5:513–519. [PubMed: 12766772]

Khokha MK, Hsu D, Brunet LJ, Dionne MS, Harland RM. Gremlin is the BMP antagonist required for maintenance of Shh and Fgf signals during limb patterning. Nat Genet. 2003; 34:303–307. [PubMed: 12808456]

Kimura S, Shiota K. Sequential changes of programmed cell death in developing fetal mouse limbs and its possible roles in limb morphogenesis. J Morphol. 1996; 229:337–346. [PubMed: 8765811]

Kuss P, Villavicencio-Lorini P, Witte F, Klose J, Albrecht AN, Seemann P, Hecht J, Mundlos S. Mutant Hoxd13 induces extra digits in a mouse model of synpolydactyly directly and by decreasing retinoic acid synthesis. J Clin Invest. 2009; 119:146–156. [PubMed: 19075394]

Lallemand Y, Nicola MA, Ramos C, Bach A, Clement CS, Robert B. Analysis of Msx1; Msx2 double mutants reveals multiple roles for Msx genes in limb development. Development. 2005; 132:3003–3014. [PubMed: 15930102]

Lewandoski M, Sun X, Martin GR. Fgf8 signalling from the AER is essential for normal limb development. Nat Genet. 2000; 26:460–463. [PubMed: 11101846]

Lewandowski JP, Pursell TA, Rabinowitz AH, Vokes SA. Manipulating gene expression and signaling activity in cultured mouse limb bud cells. Dev Dyn. 2014

Li Q, Lewandowski JP, Powell MB, Norrie JL, Cho SH, Vokes SA. A Gli silencer is required for robust repression of gremlin in the vertebrate limb bud. Development. 2014; 141:1906–1914. [PubMed: 24700818]

Litingtung Y, Dahn RD, Li Y, Fallon JF, Chiang C. Shh and Gli3 are dispensable for limb skeleton formation but regulate digit number and identity. Nature. 2002; 418:979–983. [PubMed: 12198547]

Livak KJ, Schmittgen TD. Analysis of relative gene expression data using real-time quantitative PCR and the 2(−Delta Delta C(T)) Method. Methods. 2001; 25:402–408. [PubMed: 11846609]

Ljosa V, Carpenter AE. Introduction to the quantitative analysis of two-dimensional fluorescence microscopy images for cell-based screening. PLoS Comput Biol. 2009; 5:e1000603. [PubMed: 20041172]

Logan M, Martin JF, Nagy A, Lobe C, Olson EN, Tabin CJ. Expression of Cre Recombinase in the developing mouse limb bud driven by a Prxl enhancer. Genesis. 2002; 33:77–80. [PubMed: 12112875]

Lopez-Rios J, Speziale D, Robay D, Scotti M, Osterwalder M, Nusspaumer G, Galli A, Hollander GA, Kmita M, Zeller R. GLI3 constrains digit number by controlling both progenitor proliferation and BMP-dependent exit to chondrogenesis. Dev Cell. 2012; 22:837–848. [PubMed: 22465667]

Lu P, Minowada G, Martin GR. Increasing Fgf4 expression in the mouse limb bud causes polysyndactyly and rescues the skeletal defects that result from loss of Fgf8 function. Development. 2006; 133:33–42. [PubMed: 16308330]

Mariani FV, Ahn CP, Martin GR. Genetic evidence that FGFs have an instructive role in limb proximal-distal patterning. Nature. 2008; 453:401–405. [PubMed: 18449196]

Michos O, Panman L, Vintersten K, Beier K, Zeller R, Zuniga A. Gremlin-mediated BMP antagonism induces the epithelial-mesenchymal feedback signaling controlling metanephric kidney and limb organogenesis. Development. 2004; 131:3401–3410. [PubMed: 15201225]

NIH-PA Author Manuscript NIH-PA Author Manuscript NIH-PA Author Manuscript

Milaire J, Rooze M. Hereditary and Induced Modifications of the Normal Necrotic Patterns in the Developing Limb Buds of the Rat and Mouse - Facts and Hypotheses. Arch Biol. 1983; 94:459–490.

Minowada G, Jarvis LA, Chi CL, Neubuser A, Sun X, Hacohen N, Krasnow MA, Martin GR. Vertebrate Sprouty genes are induced by FGF signaling and can cause chondrodysplasia when overexpressed. Development. 1999; 126:4465–4475. [PubMed: 10498682]

Nguyen MT, Zhu J, Nakamura E, Bao X, Mackem S. Tamoxifen-dependent, inducible Hoxb6CreERT recombinase function in lateral plate and limb mesoderm, CNS isthmic organizer, posterior trunk neural crest, hindgut, and tailbud. Dev Dyn. 2009; 238:467–474. [PubMed: 19161221]

Oh CD, Maity SN, Lu JF, Zhang J, Liang S, Coustry F, de Crombrugghe B, Yasuda H. Identification of SOX9 interaction sites in the genome of chondrocytes. PLoS One. 2010; 5:e10113. [PubMed: 20404928]

Ovchinnikov DA, Selever J, Wang Y, Chen YT, Mishina Y, Martin JF, Behringer RR. BMP receptor type IA in limb bud mesenchyme regulates distal outgrowth and patterning. Dev Biol. 2006; 295:103–115. [PubMed: 16630606]

Pajni-Underwood S, Wilson CP, Elder C, Mishina Y, Lewandoski M. BMP signals control limb bud interdigital programmed cell death by regulating FGF signaling. Development. 2007; 134:2359–2368. [PubMed: 17537800]

Perez WD, Weller CR, Shou S, Stadler HS. Survival of Hoxa13 homozygous mutants reveals a novel role in digit patterning and appendicular skeletal development. Dev Dyn. 2010; 239:446–457. [PubMed: 20034107]

Pignatti E, Zeller R, Zuniga A. To BMP or not to BMP during vertebrate limb bud development. Semin Cell Dev Biol. 2014

Pizette S, Abate-Shen C, Niswander L. BMP controls proximodistal outgrowth, via induction of the apical ectodermal ridge, and dorsoventral patterning in the vertebrate limb. Development. 2001; 128:4463–4474. [PubMed: 11714672]

Pizette S, Niswander L. BMPs negatively regulate structure and function of the limb apical ectodermal ridge. Development. 1999; 126:883–894. [PubMed: 9927590]

Rabinowitz AH, Vokes SA. Integration of the transcriptional networks regulating limb morphogenesis. Dev Biol. 2012; 368:165–180. [PubMed: 22683377]

Rosello-Diez A, Arques CG, Delgado I, Giovinazzo G, Torres M. Diffusible signals and epigenetic timing cooperate in late proximo-distal limb patterning. Development. 2014; 141:1534–1543. [PubMed: 24598165]

Scherz PJ, Harfe BD, McMahon AP, Tabin CJ. The limb bud Shh-Fgf feedback loop is terminated by expansion of former ZPA cells. Science. 2004; 305:396–399. [PubMed: 15256670]

Sekiya I, Tsuji K, Koopman P, Watanabe H, Yamada Y, Shinomiya K, Nifuji A, Noda M. SOX9 enhances aggrecan gene promoter/enhancer activity and is up-regulated by retinoic acid in a cartilage-derived cell line, TC6. J Biol Chem. 2000; 275:10738–10744. [PubMed: 10753864]

Selever J, Liu W, Lu MF, Behringer RR, Martin JF. Bmp4 in limb bud mesoderm regulates digit pattern by controlling AER development. Dev Biol. 2004; 276:268–279. [PubMed: 15581864]

Sheth R, Marcon L, Bastida MF, Junco M, Quintana L, Dahn R, Kmita M, Sharpe J, Ros MA. Hox genes regulate digit patterning by controlling the wavelength of a Turing-type mechanism. Science. 2012; 338:1476–1480. [PubMed: 23239739]

Srinivas S, Watanabe T, Lin CS, William CM, Tanabe Y, Jessell TM, Costantini F. Cre reporter strains produced by targeted insertion of EYFP and ECFP into the ROSA26 locus. BMC Dev Biol. 2001; 1:4. [PubMed: 11299042]

Stadler HS, Higgins KM, Capecchi MR. Loss of Eph-receptor expression correlates with loss of cell adhesion and chondrogenic capacity in Hoxa13 mutant limbs. Development. 2001; 128:4177–4188. [PubMed: 11684655]

Sun X, Mariani FV, Martin GR. Functions of FGF signalling from the apical ectodermal ridge in limb development. Nature. 2002; 418:501–508. [PubMed: 12152071]

Swiatek PJ, Gridley T. Perinatal lethality and defects in hindbrain development in mice homozygous for a targeted mutation of the zinc finger gene Krox20. Genes Dev. 1993; 7:2071–2084. [PubMed: 8224839]

NIH-PA Author Manuscript

NIH-PA Author Manuscript

NIH-PA Author Manuscript

te Welscher P, Zuniga A, Kuijper S, Drenth T, Goedemans HJ, Meijlink F, Zeller R. Progression of vertebrate limb development through SHH-mediated counteraction of GLI3. Science. 2002; 298:827–830. [PubMed: 12215652]

ten Berge D, Brugmann SA, Helms JA, Nusse R. Wnt and FGF signals interact to coordinate growth with cell fate specification during limb development. Development. 2008; 135:3247–3257. [PubMed: 18776145]

Towers M, Mahood R, Yin Y, Tickle C. Integration of growth and specification in chick wing digit-patterning. Nature. 2008; 452:882–886. [PubMed: 18354396]

Vargesson N, Kostakopoulou K, Drossopoulou G, Papageorgiou S, Tickle C. Characterisation of hoxa gene expression in the chick limb bud in response to FGF. Dev Dyn. 2001; 220:87–90. [PubMed: 11146510]

Ventura A, Kirsch DG, McLaughlin ME, Tuveson DA, Grimm J, Lintault L, Newman J, Reczek EE, Weissleder R, Jacks T. Restoration of p53 function leads to tumour regression in vivo. Nature. 2007; 445:661–665. [PubMed: 17251932]

Verheyden JM, Lewandoski M, Deng C, Harfe BD, Sun X. Conditional inactivation of Fgfr1 in mouse defines its role in limb bud establishment, outgrowth and digit patterning. Development. 2005; 132:4235–4245. [PubMed: 16120640]

Verheyden JM, Sun X. An Fgf/Gremlin inhibitory feedback loop triggers termination of limb bud outgrowth. Nature. 2008; 454:638–641. [PubMed: 18594511]

Vokes SA, Ji H, Wong WH, McMahon AP. A genome-scale analysis of the cis- regulatory circuitry underlying sonic hedgehog-mediated patterning of the mammalian limb. Genes Dev. 2008; 22:2651–2663. [PubMed: 18832070]

Zhang P, Jimenez SA, Stokes DG. Regulation of human COL9A1 gene expression. Activation of the proximal promoter region by SOX9. J Biol Chem. 2003; 278:117–123. [PubMed: 12399468]

Zhu J, Nakamura E, Nguyen MT, Bao X, Akiyama H, Mackem S. Uncoupling Sonic hedgehog control of pattern and expansion of the developing limb bud. Dev Cell. 2008; 14:624–632. [PubMed: 18410737]

NIH-PA Author Manuscript

NIH-PA Author Manuscript

NIH-PA Author Manuscript

HIGHLIGHTS

- We generated an inducible allele *Gremlin* that results in reduced BMP activity
- Inhibiting mesodermal BMPs between E10.5–11.5 results in polydactylous limbs
- Inhibiting mesodermal BMPs results in persistent FGF signaling
- Digit rays are specified normally but have delays in chondrogenic differentiation

NIH-PA Author Manuscript
NIH-PA Author Manuscript
NIH-PA Author Manuscript

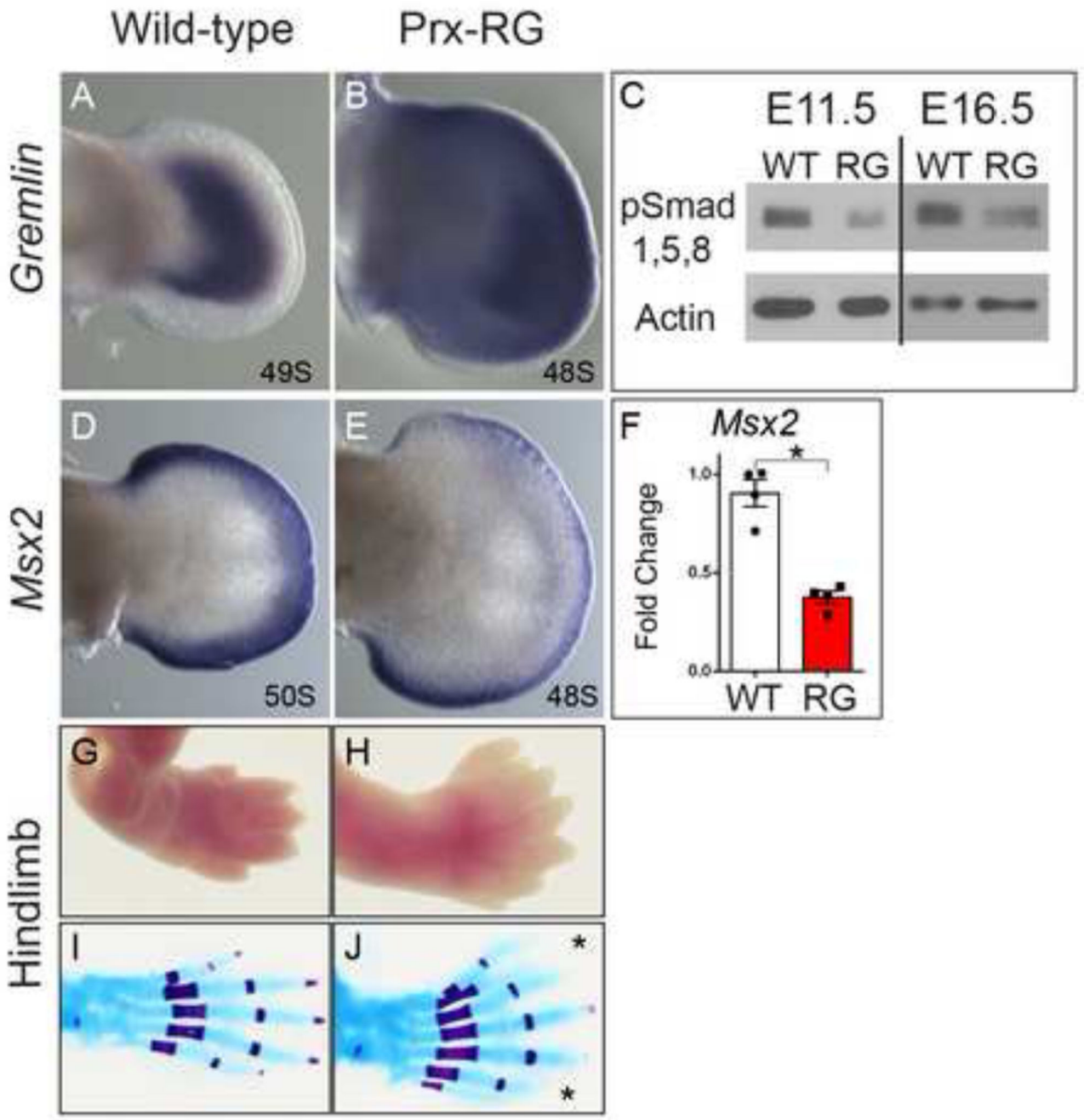

Figure 1. Ectopic Gremlin inhibits BMP signaling resulting in hindlimb polydactyly

In-situ hybridization for *Gremlin* at E11.75 (A–B). Note *Gremlin* expression throughout the limb mesenchyme in the Prx-RG (B). Prx-RG hindlimbs have reduced *pSMAD*1/5/8 levels on Western blots at 11.5 (53% reduction P=.0001) and continue to have reduced levels in E16.5 autopods (29% reduction P=0.04; normalized to beta-actin levels). *In-situ* hybridization for *Msx2* at E11.75 showing decreased expression in Prx-RG limb mesenchyme (D, E). There is a corresponding ~70% decrease in *Msx2* levels (P<0.05) (F).

E18.5 Prx-RG hindlimbs have fully penetrant polydactylous hindlimbs along with soft tissue syndactyly (G–J). Error bars indicate the standard error of mean (F).

NIH-PA Author Manuscript
NIH-PA Author Manuscript
NIH-PA Author Manuscript

NIH-PA Author Manuscript
NIH-PA Author Manuscript
NIH-PA Author Manuscript

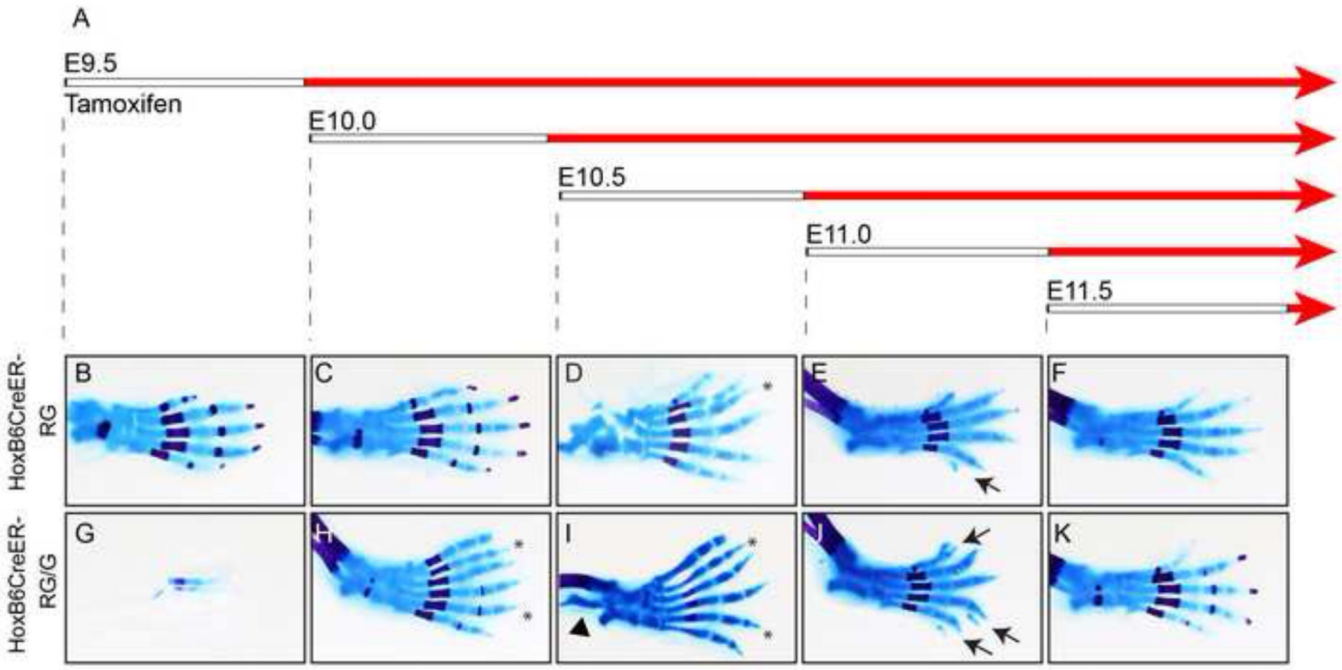

Figure 2. Mesodermal BMP signaling regulates digit number between E10.5 and E11.5

(A) Pregnant mice were injected with tamoxifen when embryos were at the specified time-points (white bars). Effective activation of ectopic *Gremlin* occurs approximately 8–12 hours later (red bars). Embryos were analyzed by skeletal preparation at E18.5 (B–K). Asterisks indicate polydactylous digits, arrows indicate nubs, and the arrowhead in I indicates defects in the tibia and fibula. The tibia and fibula were removed from the autopod in D prior to imaging. Images are representative of the most common phenotype with a minimum of three embryos per condition (Table S3) except for panel C (n=1). At all time-points, wild type siblings (containing RG or RG/G but no HoxB6CreER) from tamoxifen-injected litters had normal limbs and digits (Table S3).

NIH-PA Author Manuscript
NIH-PA Author Manuscript
NIH-PA Author Manuscript

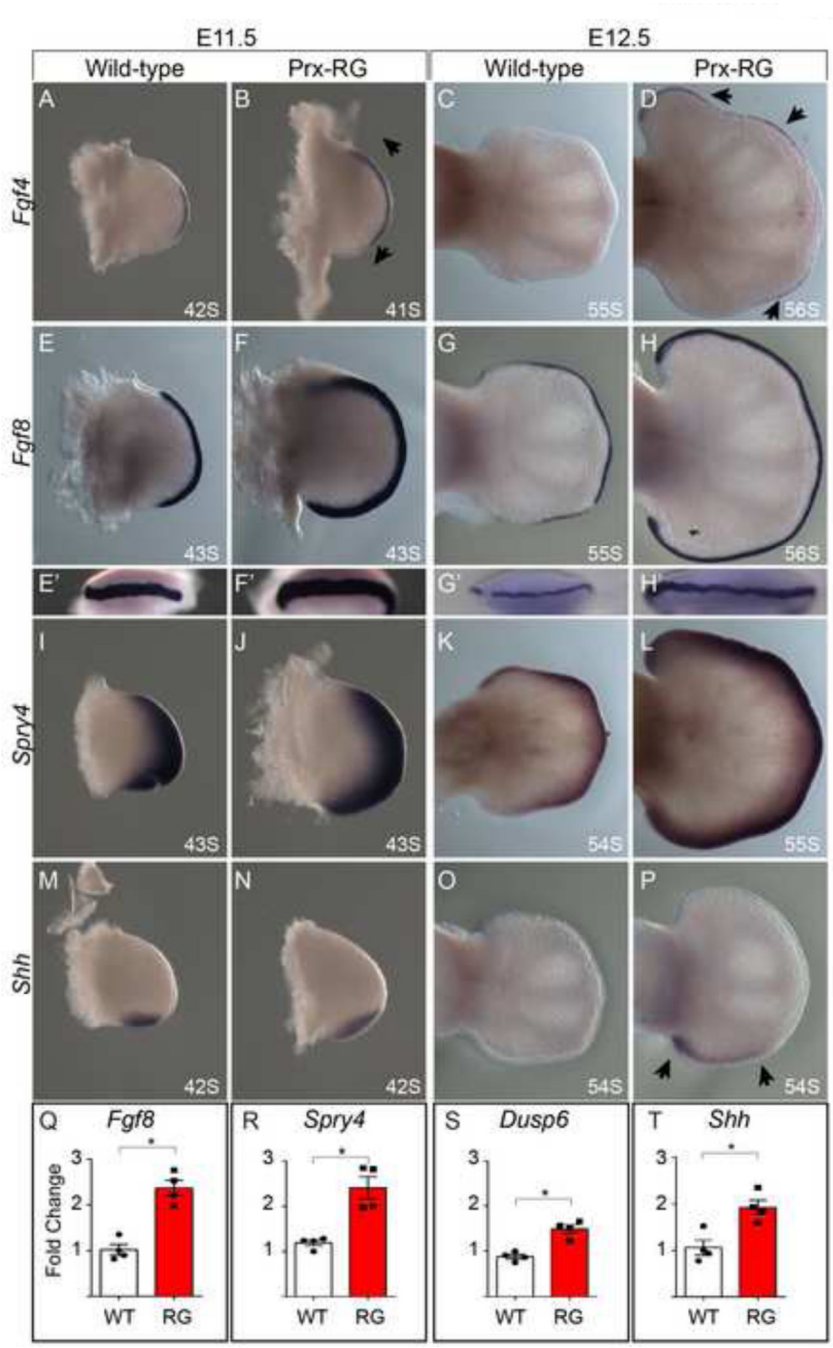

Figure 3. RG hindlimbs have elevated, persistent FGF signaling

In-situ hybridizations with the somite stage indicated at bottom right (A–P) for *Fgf4* (A–D), *Fgf8* (E–H'), *Spry4* (I–L) and *Shh* (M–P) at E11.5 and E12.5. *Fgf4* is expanded in both the anterior and posterior domains at E11.5 (B, arrows) with persistent and ectopic expression at E12.5 after expression is absent from wild type controls (D, arrow heads). Similar expression is seen for *Fgf8* (E-H') and for the FGF responsive gene *Spry4* levels (I–L). *Shh* is expanded in the proximal to distal domain at E11.5 and its expression is sustained at E12.5 in an expanded proximal/distal domain (arrows). Quantitative RT-PCR analysis of

NIH-PA Author Manuscript

NIH-PA Author Manuscript

NIH-PA Author Manuscript

Fgf8, *Spry4*, *Dusp6*, and *Shh* at E11.75 indicate significant increases (asterisk indicates $P<0.05$) in expression levels in Prx-RG hindlimbs. Error bars indicate the standard error of mean (Q–T).

NIH-PA Author Manuscript
NIH-PA Author Manuscript
NIH-PA Author Manuscript

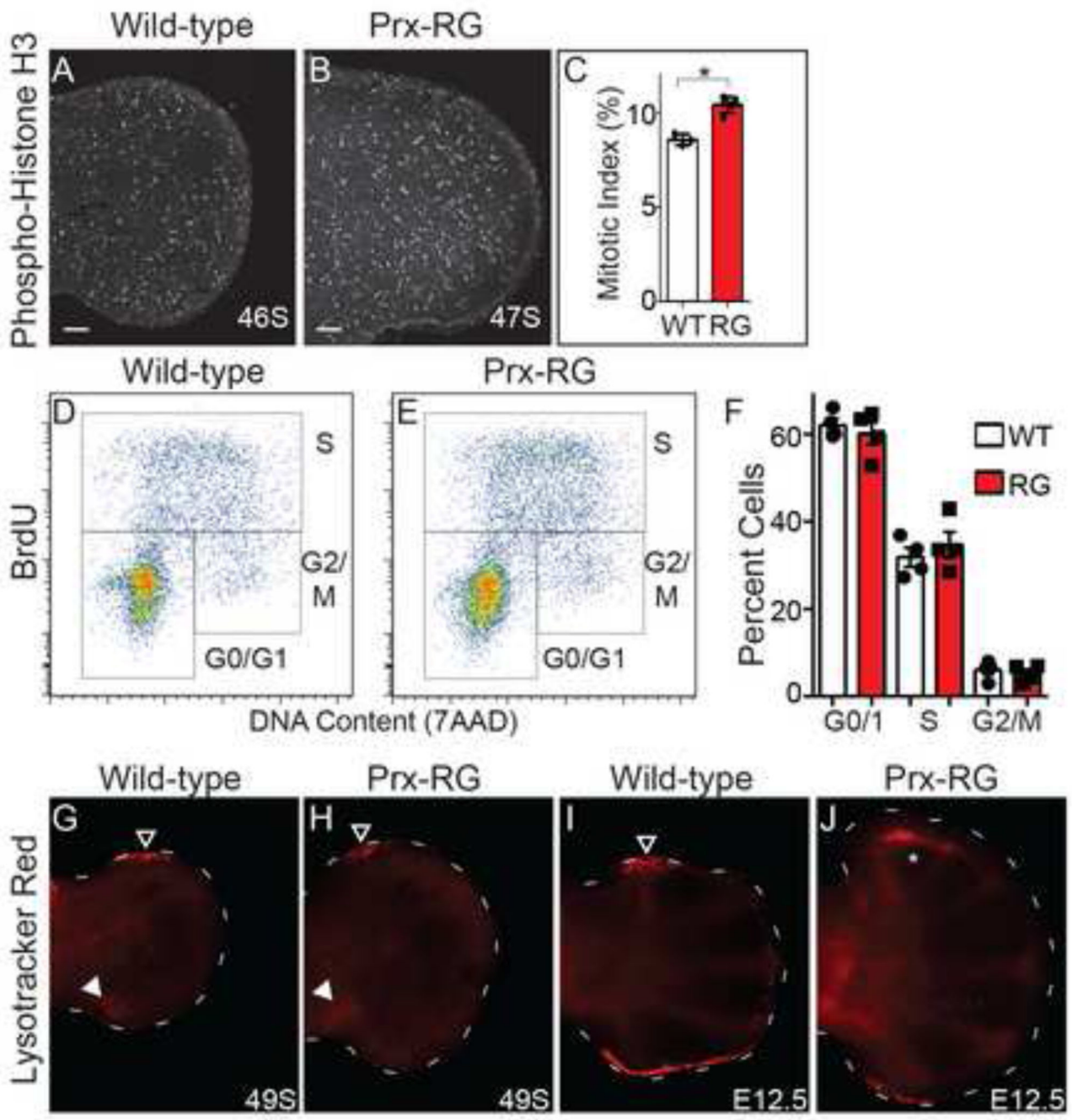

Figure 4. BMP inhibition results in increased proliferation and cell survival

Sections were immunostained for the presence of phosphohistone H3 (PHH3) on dorsal-ventral sections through the hindlimb autopod of E11.5 embryos (A, B). There is a significant increase in the percentage of PHH3 positive cells in RG ($P<0.05$) (C). Cell cycle analysis of WT and Prx-RG hindlimbs at E11.75 by flow cytometry gated into G0/G1, S, and G2,M phases (D,E). The average percentages of cells for each population (n=4) (F) are unchanged between WT and Prx-RG. Whole-mount staining for Lysotracker Red on hindlimbs at E11.75 (G,H) and E12.5 (I,J). Filled arrowheads in G,H indicate the posterior

NIH-PA Author Manuscript

NIH-PA Author Manuscript

NIH-PA Author Manuscript

necrotic zone. Open arrowheads (G-I) indicate the anterior necrotic zone. The altered domain of anterior apoptosis in J is indicated by the white asterisk. Staging in somites (S) or embryonic day (E) is indicated on bottom right. Scale bars on images A,B indicate 100μM. Error bars indicate the standard error of mean (C,F).

NIH-PA Author Manuscript

NIH-PA Author Manuscript

NIH-PA Author Manuscript

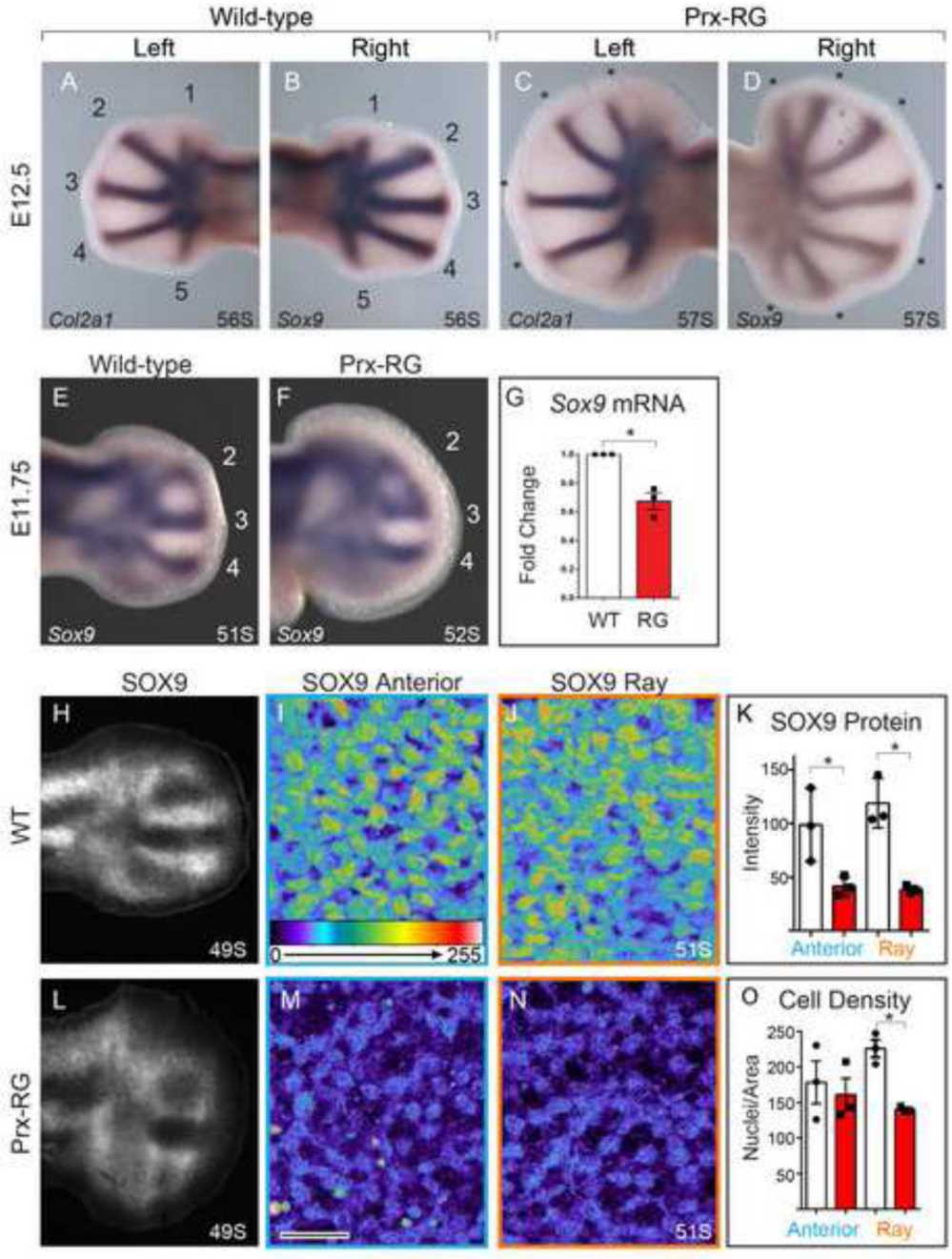

Figure 5. BMP inhibition delays chondrogenesis and reduces Sox9

In-situ hybridization for *Col2a1* and *Sox9* on contralateral hindlimbs from the same embryo (A–D). The wild type embryo has 5 condensed *Col2a1* positive digits as well as 5 *Sox9* positive digit rays while the RG embryo has more *Sox9* expressing rays than *Col2a1* expressing rays (asterisks indicate polydactylous digit rays - the posterior *Col2a1* domain (D) is not considered a digit because it has not yet fully expanded distally). *In-situ* hybridization for *Sox9* at E11.75 (E–F). Quantitative RT-PCR for *Sox9* normalized to *Gapdh* (G) shows a 33% decrease in expression in Prx-RG hindlimbs at E11.75 ($P<0.05$). Sections

NIH-PA Author Manuscript

NIH-PA Author Manuscript

NIH-PA Author Manuscript

immunostained for SOX9 and visualized epifluorescent light microscope (H,L). Additional 40x single plane confocal images (I,J, M and N; Scale bar= 20μm) show SOX9 positive cells with intensity indicated on a scale of 0–255 on comparable regions of WT and RG hindlimbs. The blue box (I,M) shows the anterior, uncondensed portion of the limb bud while the orange box (J,N) shows the condensing middle digit ray (sections in I,J,M,N are from different embryos than H,L). As reflected in the images, there is a significant reduction in SOX9 fluorescent intensity (K). There is also a significant reduction in nuclear density in the middle digit ray in Prx-RG limbs ($P<0.05$) while there is no difference in the density of uncondensed Sox9 expressing cells in the anterior limb (O). Data points on graphs indicate measurements from independent embryos. Where applicable, somite stages are indicated in the bottom right. Error bars indicate the standard error of mean (G,K,O).

NIH-PA Author Manuscript
NIH-PA Author Manuscript
NIH-PA Author Manuscript

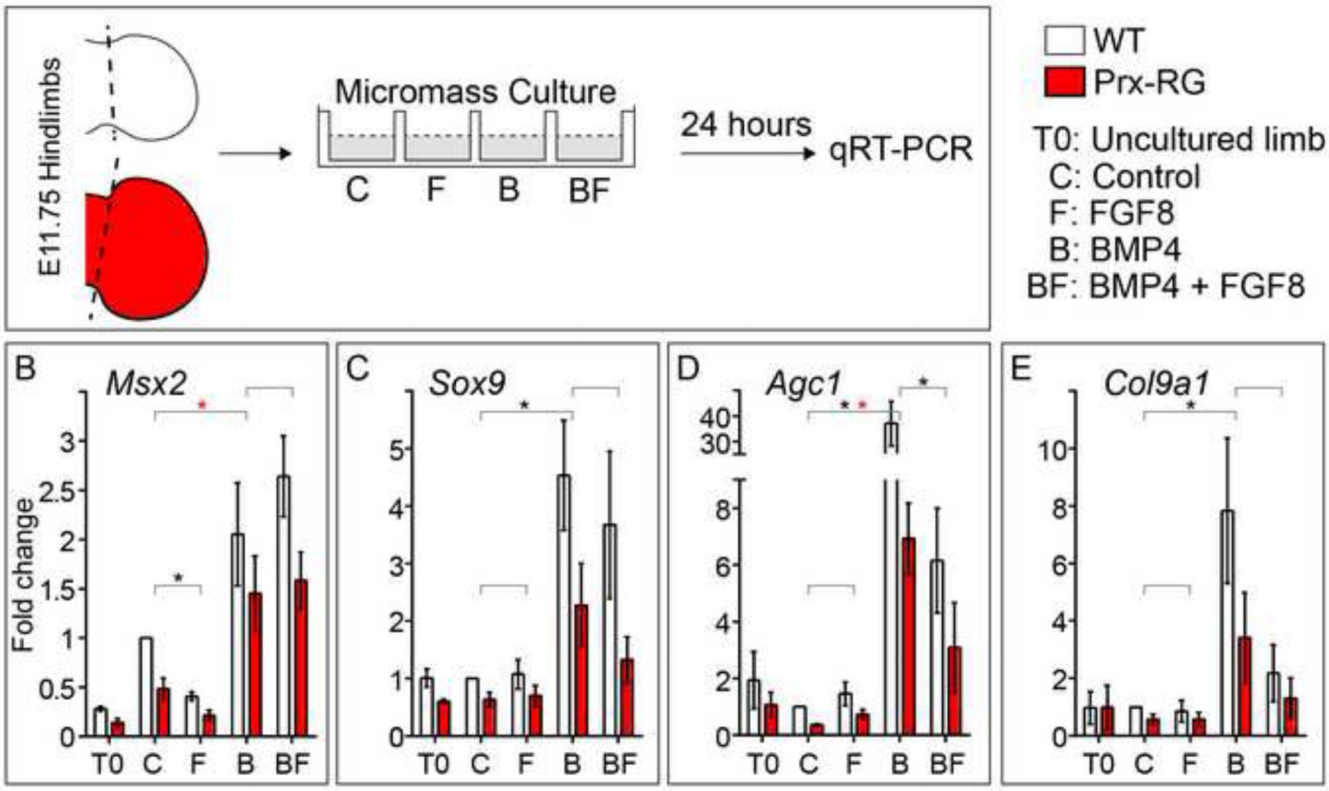

Figure 6. Limb bud cultures show a delay in differentiation of cells lacking BMP

Hindlimb autopods from WT and Prx-RG embryos were dissected and dissociated for a micromass culture (A) in either control media or media supplemented with Fgf8, BMP4, or Fgf8 and BMP4. Cultures were analyzed after 24 hours by qRT-PCR (B–E) for *Msx2* (n=5), *Sox9* (n=5), *Agc1* (n=5) and *Col9a1* (n=4). All samples were normalized to *Gapdh*. Brackets indicate pairs that were compared by statistical analysis. Statistical significance ($P<0.05$) is indicated by a black asterisk between WT samples and a red asterisk between RG samples. Analysis of WT and RG *Sox9* at T0 depicts that same data shown in Figure 5G. Error bars indicate the standard error of mean (B–E).

NIH-PA Author Manuscript
NIH-PA Author Manuscript
NIH-PA Author Manuscript

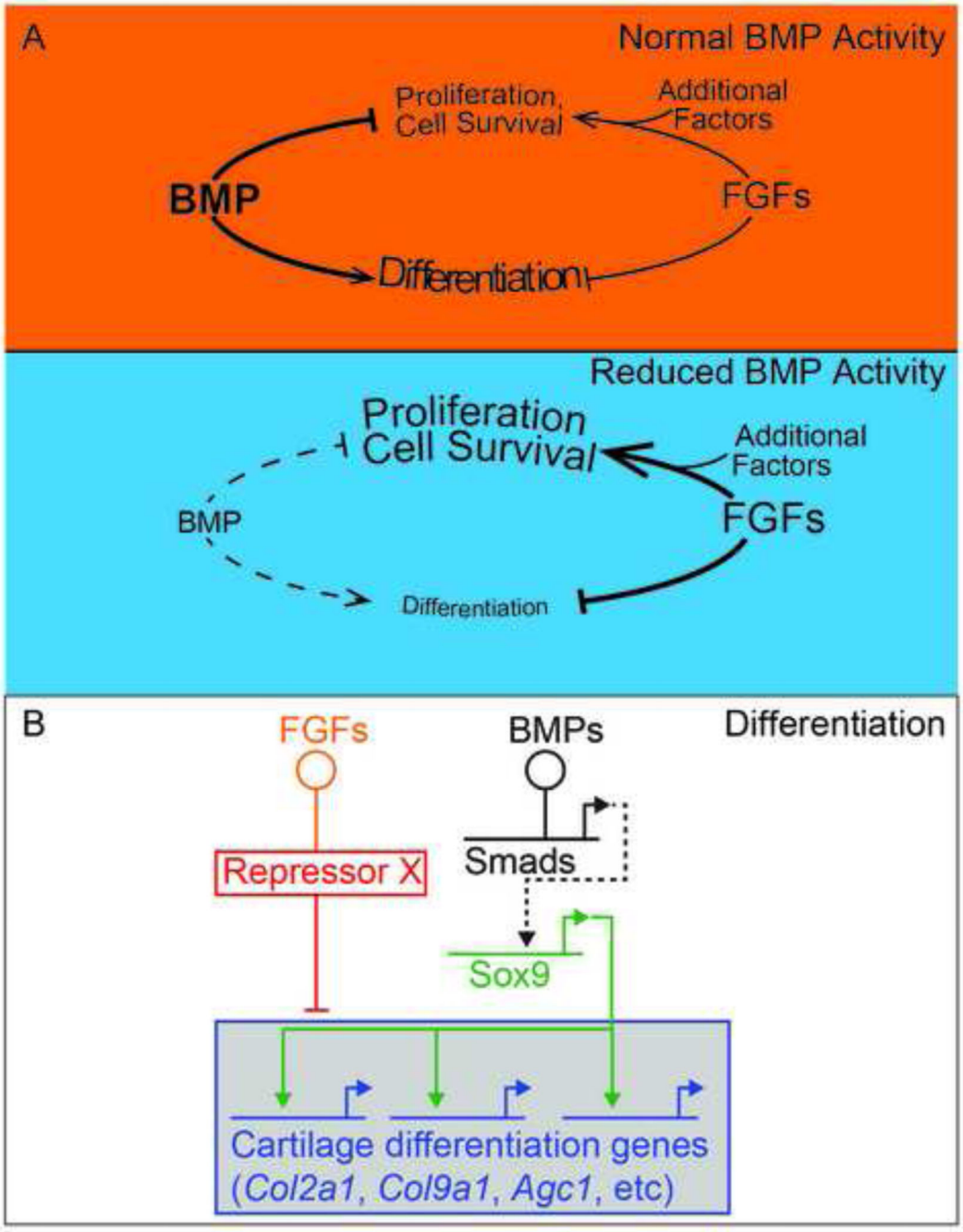

Figure 7. Model depicting the roles for BMP in digit chondrogenesis

(A) Under wild type conditions, increasing levels of BMP activity over development promote differentiation (chondrogenesis) and suppress proliferation. During this time, normal levels of FGFs promote proliferation by amplifying Shh and Wnt signaling (represented as 'additional factors'), until their downregulation at the end of limb specification. When BMP levels are reduced in RG hindlimbs, there is a delay in chondrogenic differentiation. FGF levels persist after they are normally downregulated. This maintains the high level of proliferation seen in earlier limb mesoderm and inhibits normal

NIH-PA Author Manuscript

NIH-PA Author Manuscript

NIH-PA Author Manuscript

apoptotic domains. Maintaining proliferation inhibits Sox9 expression and entry into a chondrogenic pathway and independently inhibits later chondrogenic differentiation. (B) Gene regulatory network underlying digit chondrogenesis. Threshold levels of BMPs activate *Sox9* in a dose-dependent fashion through Smads in a direct or indirect fashion (dashed lines). SOX9, in turn, activates markers of differentiated chondrocytes. Amplified FGFs inhibit chondrogenesis both repressing differentiation genes in a parallel pathway by regulating a repressor.